Regular Article

PHYSICAL CHEMISTRY RESEARCH
Published by the
Iranian Chemical Society
www.physchemres.org
info@physchemres.org

Phys. Chem. Res., Vol. 8, No. 3, 471-496, September 2020
DOI: 10.22036/pcr.2020.211346.1707

Prediction of DES' Vapor Pressure Using a New Corresponding State Model

F. Esmaeilzadeh[a,*], F. Zarei[a], S.M. Mousavi[a] and G.R. Vakili-Nezhaad[b]

[a]*Department of Chemical and Petroleum Engineering, School of Chemical and Petroleum Engineering, Enhanced Oil and Gas Recovery Institute, Advanced Research Group for Gas Condensate Recovery, Shiraz University, Shiraz 7134851154, Iran*

[b]*Petroleum and Chemical Engineering Department, College of Engineering, Sultan Qaboos University, Muscat 123, Oman*

(Received 10 December 2019, Accepted 25 April 2020)

Application of deep eutectic solvents (DES) in industrial chemical processes has been improved during the last decades. In this work, vapor pressures of 13 classes of DESs (DES 1-13) based on 5 salts and 7 hydrogen bond donors with various combinations of molar ratio were used between 343-393 K. The vapor pressures of the pure and aqueous solutions of DESs were calculated by different equations of state based on "φ-φ" or "γ-φ" γ-φ approaches. Additionally, the Voutsas and Wagner models as corresponding-state models were modified to predict the vapor pressure of the pure and aqueous solutions of DES with the total average absolute relative deviations of 7.03, 9.08% and 5.47, 7.15%, respectively. Moreover, the validity of vapor pressure calculation using the two modified models was checked using a linear equation for the average specific heat capacity of different DESs (23 classes of DESs) between 278.15-353.15 K. Results showed that the total average absolute relative deviations of the specific heat capacity of DESs, using the Modified-Voutsas and Modified-Wagner models from the experimental data, were 4.128 and 4.056%, respectively.

Keywords: Deep eutectic solvents, Vapor pressure, Corresponding state models, Equation of state, Model, Prediction, Pure compounds, Aqueous solutions

INTTRODUCTION

The traditional solvents release considerable amounts of volatile organic compounds with the toxic effects into the environment, owing to their high volatility. Many researchers have focused on attaining a new, clean, safe and healthy industrial solvent with the help of green technologies [1,2]. The green technologies proposed a new solvent which could be broadly used to minimize the air and environmental pollutions [3]. As a result, the deep eutectic solvents (DESs) were suggested by many researchers for this purpose. DESs are superior to bio-solvents and they have not the disastrous drawbacks of the conventional solvents [4,5]. Although ionic liquids (ILs) have been introduced as the green solvents in the literature, there are studies illustrating the toxicity of ILs [3]. So, the risks ofILs, their high volatility and high cost led to introduce DESs as the new solvents [6]. DESs were produced by mixing an organic salt with an organic compound as a hydrogen bond donor, and displayed the properties similar to ILs [7]. These solvents have different characteristics, owing to the various cation and anion parts. Considerable attention has been paid to use the DESs by many researchers because of their high solvation ability, superior thermal/chemical stabilities, low toxicity, non-inflammable and an easy preparation method with high purity [8-10]. Moreover, the DESs have low vapor pressures. Many researchers have announced that the vapor pressure of DESs is negligible. However, the vapor pressure data of various compositions of DESs demonstrated that the mentioned issue is incorrect. The vapor pressure is a paramount parameter in the environmental study. The transport phenomena and distribution of the toxic chemicals in water, air and soil were studied by the vapor pressure information

*Corresponding author. E-mail: esmaeilzadeh95@gmail.com

[11]. Also, the viscosity of a liquid, the enthalpy of vaporization and the air-water partition coefficient were estimated by the vapor pressure data. So, the vapor pressure has a substantial role in the design, optimization and control of the processes [12]. Moreover, vapor pressure has a key role in many industrial applications like the absorption of heat pump, water desalination and organic solvent recycling [13]. On the other hand, vapor pressure is introduced as an important physicochemical property that has a considerable effect on the vapor-liquid and solid-vapor phase equilibria [14]. So, the vapor pressure of DESs should be comprehensively investigated as an essential effective parameter.

However, few experimental and theoretical works have been performed on the vapor pressure of DESs. Nevertheless, besides the experimental data and empirical and theoretical models, the Clausius-Clapeyron equation is a valid method for the prediction of vapor pressure as shown in Eq. (1) [15]:

$$\frac{dp}{dT} = \frac{\Delta H}{T\,(V_g - V_L)} \tag{1}$$

This equation is based on three assumptions:

1. The heat of vaporization is temperature-independent.
2. The vapor phase is considered as an ideal gas.
3. The volume occupied by liquid is negligible as compared to that occupied by the vapor in the saturation pressure [16].

However, the assumptions of Clausius-Clapeyron equation are not true conformity for different compositions of DESs. In addition, the Clausius-Clapeyron equation is dependent on the enthalpy of vaporization, and the gas and liquid volume data. So, the Clausius-Clapeyron equation is not a fast and easy method to predict the vapor pressure of DESs. In this work, the equilibrium concept, equation of states (EoSs), Clausius-Clapeyron equation, corresponding state theory, and group contribution method were used to present an efficient model for the prediction of pure and aqueous solutions of DESs' vapor pressure.

MODELLING AND CALCULATIONS

Systems

In this work, 12 deep eutectic solvents were studied by the combination of various molar ratios of 5 different salts and 7 different hydrogen bond donors (HBDs). Compositions of all DESs and their experimental vapor pressure ranges are given in Table 1 [17-21]. N,N-Diethylenethanol ammonium chloride ($(C_2H_5)_2NCH_2CH_2OH/HCl$), methyl triphenyl phosphonium bromide ($C_{19}H_{18}PBr$), Choline chloride ($C_5H_{14}CINO$), decanoic acid ($C_{10}H_{20}O_2$) and thymol ($C_{10}H_{14}O$) were used as the salts. Moreover, glycerol ($C_3H_8O_3$), urea (CH_4N_2O), lidocaine ($C_{14}H_{22}N_2O$), menthol ($C_{10}H_{20}O$), ethylene glycol ($C_2H_6O_2$) and malonic acid ($C_3H_4O_4$) were used as agents for the formation of hydrogen bond donors. All salts and HBDs had the purity of more than 98 wt.%. DES-1 to DES-11 are pure compounds. Also, DES-1, DES-2, DES-12 and DES-13, known as glycerine, reline, ethaline and maline, respectively, are aqueous solutions.

DESs Characterization

Group contribution method (GCM) was used to predict the critical properties of DESs including normal boiling point, critical temperature, critical pressure, critical volume, critical compressibility factor and acentric factor. The modified Lydersen-Joback-Reid model was exploited as a high-efficient model to determine the properties of salts and HBDs [22,23]. The modified Lydersen-Joback-Reid model provides the preference of rapid estimates without the need of fundamental computational resources. Since the modified Lydersen-Joback-Reid model has been employed for the compounds with high molecular weight, this model was applied for the estimation of the properties of DESs. The groups for the Modified Lydersen-Joback-Reid group contribution are shown in Table 2. The properties of compounds are estimated by Eqs. (2)-(7). Some researchers noted this model provides precise estimations of the critical properties of the organic compounds [22,23].

$$T_b(K) = A + \sum n\Delta T_b \tag{2}$$

$$T_c(K) = \frac{T_b}{B + c\sum n\Delta T_c - (\sum n\Delta T_c)^2} \tag{3}$$

$$P_c(bar) = \frac{MW}{[D + \sum n\Delta P_c]^2} \tag{4}$$

Table 1. The Deep Eutectic Solvents' (DESs') Composition and their Experimental Vapor Pressure Ranges [17-21]

Abbreviation	Molar ratio	Number of data points	Temperature (K)	Salt	HBD	Min vapor pressure (Pa)	Max vapor pressure (Pa)
DES-1	1:2	20[a]	303-343	Choline chloride	Glycerol	1786.51	29277.51
		6[b]	343-393			2.14	46.16
DES-2	1:2	40[a]	303-343	Choline chloride	Urea	1893	29398
		6[b]	343-393			0.34	2.94
DES-3	1:2	6	343-393	N,N-Diethylenethanol ammonium chloride	Glycerol	2.16	607.79
DES-4	1:2	6	343-393	N,N-Diethylenethanol ammonium chloride	Urea	0.14	6.79
DES-5	1:2	6	343-393	Methyl triphenyl phosphonium bromide	Glycerol	0.83	35.33
DES-6	1:1	5	313-373	Decanoic acid	Thymol	5.65	417.45
DES-7	2:1	12	313-373	Decanoic acid	Lidocaine	0.90	87.51
DES-8	3:1	12	313-373	Decanoic acid	Lidocaine	1.40	80.12
DES-9	4:1	12	313-373	Decanoic acid	Lidocaine	0.35	85.75
DES-10	1:1	5	313-373	Decanoic acid	Menthol	1.91	512.09
DES-11	2:1	5	313-373	Thymol	Lidocaine	2.45	312.94
DES-12	2:1	20	303-343	Choline chloride	Ethylene glycol	1599.80	29464.16
DES-13	1:1	20	303-343	Choline chloride	Malonic acid	1999.83	30064.11

[a]Aqueous solution. [b]Pure compound.

$$V_c\left(\frac{cm^3}{mol}\right) = E + \sum n\Delta V_c \tag{5}$$

$$Z_c = \frac{P_c V_c}{R T_c} \tag{6}$$

$$\omega = \frac{(T_b - 43)(T_c - 43)}{(T_c - T_b)(0.7T_c - 43)} \log\left[\frac{P_c}{P_b}\right] - \frac{(T_c - 43)}{(T_c - T_b)} \log\left[\frac{P_c}{P_b}\right] + \log\left[\frac{P_c}{P_b}\right] - 1 \tag{7}$$

where the values of A, B, C, D and E constants are equal to 198.2, 0.5703, 1.0121, 0.2573 and 6.75, respectively. Moreover, the value of P_b is considered to be 1.01325 bar. The critical properties of the mixture should be calculated by the following mixing rules [24,25]:

$$T_{cm} = \frac{1}{V^{\frac{1}{4}}} \sum_i \sum_j X_i X_j V_{cij}^{1/4} T_{cij} \tag{8}$$

Table 2. The Groups Considered for the Modified Lydersen-Joback-Reid Group Contribution [22,23]

	ΔT_{bm} (K)	ΔT_m (K)	ΔP_m (bar)	ΔV_m ($cm^3\ mol^{-1}$)
Without rings				
$-CH_3$	23.58	0.0275	0.3031	66.81
$-CH_2-$	22.88	0.0159	0.2165	57.11
>CH-	21.74	0.0002	0.1140	45.70
>C<	18.18	-0.0206	0.0539	21.78
$=CH_2$	24.96	0.0170	0.2493	60.37
=CH-	18.25	0.0182	0.1866	49.92
=C<	24.14	-0.0003	0.0832	34.90
=C=	26.15	-0.0029	0.0934	33.85
≡CH		0.0078	0.1429	43.97
≡C-		0.0078	0.1429	43.97
-OH (alcohol)	92.88	0.0723	0.1343	30.40
-O-	22.42	0.0051	0.1300	15.61
>C=O	94.97	0.0247	0.2341	69.76
-CHO	72.24	0.0294	0.3128	77.46
-COOH	169.06	0.0853	0.4537	88.60
-COO-	81.10	0.0377	0.4139	84.76
-HCOO		0.0360	0.4752	97.77
=O (others)	-10.50	0.0273	0.2042	44.03
$-NH_2$	73.23	0.0364	0.1692	49.10
>NH	50.17	0.0118	0.0322	78.96
>C-	11.74	-0.0028	0.0304	26.70
-N=	74.60	0.0172	0.1541	45.54
-CN	125.66	0.0506	0.3697	89.32
$-NO_2$	152.54	0.0448	0.4529	123.62
-F	-0.03	0.0228	0.2912	31.47
-Cl	38.13	0.0188	0.3738	62.08

Table 2. Continued

-Br	66.86	0.0124	0.5799	76.60
-I	93.84	0.0148	0.9174	100.79
With rings				
$-CH_2-$	27.15	0.0116	0.1982	51.64
>CH-	21.78	0.0081	0.1773	30.56
=CH-	26.73	0.0114	0.1693	42.55
>C<	21.32	-0.0180	0.0139	17.62
=C<	31.01	0.0051	0.0955	31.28
-O-	31.22	0.0138	0.1371	17.41
-OH (phenol)	76.34	0.0291	0.0493	-17.44
>C=O	94.97	0.0343	0.2751	59.32
>NH	52.82	0.0244	0.0724	27.61
>N-	52.82	0.0063	0.0538	25.17
-N=	57.55	-0.0011	0.0559	42.15
Other groups				
-B	-24.56	0.0352	0.0348	22.45
-P	34.86	-0.0084	0.1776	67.01
$-SO_2$	147.24	-0.0563	-0.0606	112.19

$$P_{cm} = (0.2905 - 0.0850\omega_m)\frac{RT_{cm}}{V_{cm}} \quad (9)$$

$$V_{cm} = \sum_i \sum_j \mathrm{X}_i \mathrm{X}_j V_{cij} \quad (10)$$

where

$$T_{cij} = (T_{ci}\, T_{cj})^{1/2}\, k_{ij} \quad (11)$$

$$\omega_m = \sum_i \mathrm{X}_i \omega_i \quad (12)$$

$$V_{cij} = \frac{1}{8}\left(V_{ci}^{1/3} + V_{cj}^{1/3}\right)^3 \quad (13)$$

where P_C, T_C, V_C, ω and R denote the critical pressure, critical temperature, critical volume, acentric factor and the universal gas constant. Also, m means mixture, and the value of k_{ij} is assumed to be 1 in this work.

Vapor Pressure Prediction Using Different Models

To predict vapor pressure of DESs, all experimental vapor pressure data points of DESs assessed in this work were divided into two parts. Half part of the experimental data points was used as the training data set and the remaining data points were used as the validation data set.

Voutsas model [26]. Voutsas *et al.* proposed a specified correlation for the prediction of organic compounds' vapor pressure. The Voutsas model is dependent to the normal boiling point and the reduced temperature [19,28]:

$$\ln p^s = \frac{K_f\,(8.75 + R\ln T_b)\,(18 + 0.81T_b)}{(0.97RT_b)\left(\dfrac{T - T_b}{T + 18 - 0.19T_b}\right)} \tag{14}$$

where K_f is a function of normal boiling (T_b) and the reduced temperature of DESs. So, K_f was investigated as the key part of Voutsas model.

Moreover, Eq. (18) is introduced as the objective function for evaluating the correlation of K_f,

$$obj = \frac{1}{N_p}\sum\left(\frac{P_{V_i,\exp} - P_{V_i,cal}}{P_{V_i,\exp}}\right) \tag{15}$$

where P_v is the vapor pressure of DESs, and N_p is the total number of data points. Subscripts cal and exp represent the calculated vapor pressures from the model and experiment, respectively.

Wagner model [27]. The Wagner model was introduced as a successful model to predict the phase equilibrium and vapor pressure of organic compounds. The Wagner model is dependent to the reduced temperature and acentric factor as follows:

$$\ln P_r^V = \ln P_r^{(0)} + \omega \ln P_r^{(1)} \tag{16}$$

where

$$\ln P_r^{10)} = \frac{1}{T_r}[A_1(1 - T_r) + A_2(1 - T_r)^{1.5} + A_3(1 - T_r)^3 + A_4(1 - T_r)^6] \tag{17}$$

$$\ln P_r^{(1)} = \frac{1}{T_r}[B_1(1 - T_r) + B_2(1 - T_r)^{1.5} + B_3(1 - T_r)^3 + B_4(1 - T_r)^6] \tag{18}$$

However, their constants are unknown for all substances. So, the coefficients of the Wagner model were determined for DESs as heavy compounds. For this propose, Eq. (19) is considered as the objective function to obtain the Wagner model coefficients.

$$obj\ \frac{1}{N_p}\sum\left(\frac{\ln p_r^{V_i,\exp} - \ln p_r^{V_i,cal}}{\ln p_r^{V_i,\exp}}\right) \tag{19}$$

Moreover, an adjustable correlation was coupled with the Wagner model to increase the model accuracy.

Equation of state. The equation of state was discussed as a reliable strategy to determine the characterization of different saturation properties including bubble-point pressure and dew-point pressure. However, the vapor pressure, as well as the phase equilibrium concept was predicted by the equation of states. Therefore, this procedure was introduced as an iterative method to calculate the vapor pressure. The fundamental correlation of two-phase equilibrium is as follows:

$$f_i^l = f_i^V \tag{20}$$

where

$$f_i^V = \hat{\varphi}_i^V\, y_i\, P \tag{21}$$

$$f_i^l = x_i\,\gamma_i\, f_i = \hat{\varphi}_i^l\, \mathrm{X}_i\, P \tag{22}$$

where $\hat{\varphi}_i^V$ and $\hat{\varphi}_i^l$ or γ_i are obtained from an EoS. However, it should be noted that the vapor pressure prediction by EoSs is a fairly complex approach. To overcome this problem, a more efficient iterative method was introduced to simplify the computational steps as shown in Fig. 1. According to Fig. 1, the vapor pressure of DESs was investigated to determine the equilibrium state. Finally, several EoSs including Esmaeilzadeh-Roshanfekr (ER), Soave-Redlich-Kwong (SRK), Peng-Robinson (PR) and PR-Twu were employed to estimate the vapor pressure of DESs 1 to 5. Moreover, they were compared with the corresponding state models with various deviation indexes.

Prediction of Specific Heat Capacity Using the Modified Models

The first step for the prediction of specific heat capacity using the modified models is to collect the experimental data for different classes of fatty compounds including

Table 3. Deep Eutectic Solvents (DESs) Composition [28-31]

Abbreviation	Molar ratio	Salt	HBD	Water mole fraction
DES-12	1:2	Choline chloride	Ethylene glycol	-
DES-14	1:1.98	Choline chloride	Ethylene glycol	0.3
DES-15	1:2:3	Malic acid	Betaine	0.5
DES-16	1:2	Choline chloride	Triethylene glycol	-
DES-17	1:1	Choline chloride	Malonic acid	-
DES-18	1:2	Choline chloride	Oxalic acid	-
DES-19	1:3	Choline chloride	Phenol	-
DES-20	1:3	Tetrabutyle ammonium chloride	Ethylene glycol	-
DES-21	1:4	Methyltriphynele phosphonium bromide	Ethylene glycol	-
DES-22	1:5	Tetrabutyle ammonium chloride	Glycerol	0.3
DES-23	1:5	Tetrabutyle ammonium chloride	Glycerol	0.5
DES-24	1:5	Tetrabutyle ammonium chloride	Glycerol	0.7
DES-25	1:5	Tetrabutyle ammonium chloride	Glycerol	0.9
DES-26	1:1	Tetrabutyle ammonium chloride	Triethylene glycol	0.3
DES-27	1:1	Tetrabutyle ammonium chloride	Triethylene glycol	0.5
DES-28	1:1	Tetrabutyle ammonium chloride	Triethylene glycol	0.7
DES-29	1:1	Tetrabutyle ammonium chloride	Triethylene glycol	0.9
DES-30	1:3	Tetrabutyle ammonium chloride	Ethylene glycol	-
DES-31	1:3	Tetrabutyle ammonium chloride	Ethylene glycol	0.1
DES-32	1:3	Tetrabutyle ammonium chloride	Ethylene glycol	0.3
DES-33	1:3	Tetrabutyle ammonium chloride	Ethylene glycol	0.5
DES-34	1:3	Tetrabutyle ammonium chloride	Ethylene glycol	0.7
DES-35	1:3	Tetrabutyle ammonium chloride	Ethylene glycol	0.9

DES-12 to DES-35 [28-31]. A total of 476 experimental data of DESs′specific heat capacity have been found as shown in Table 1. It can be noted that the data bank covers a wide range of temperature (278.15-353.15 K). Also, the modified vapor pressure models, proposed by the authors, were employed for DES-12 to DES-35 and DES-2 using Clausius-Clapeyron equation, which confirm the accuracy of vapor pressure calculations using the Modified-Wagner model as well as the Modified-Voutsas model.

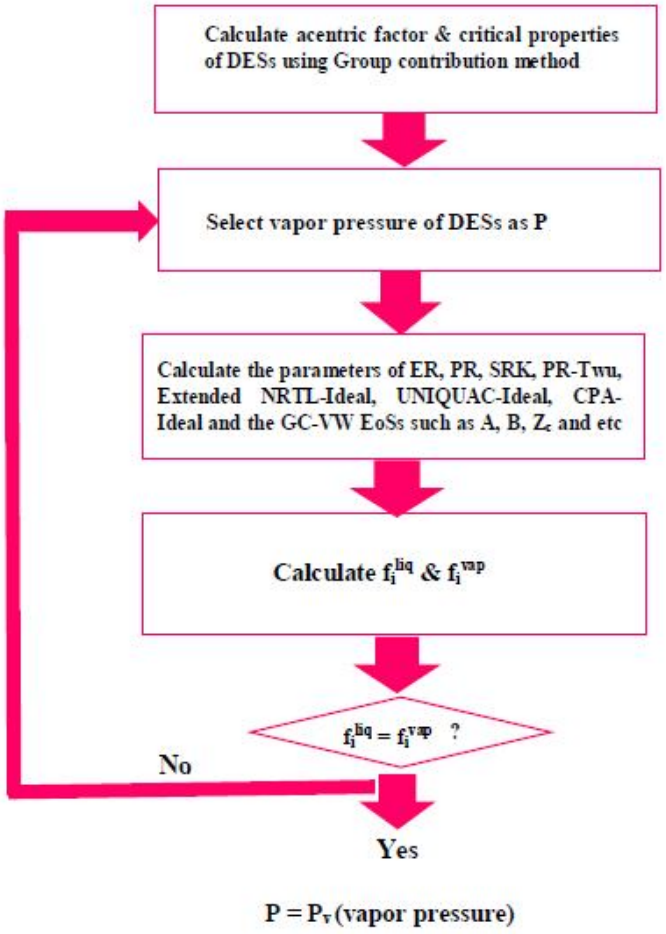

Fig. 1. Procedure of vapor pressure prediction by the EoSs assessed in this work.

Table 4. Genetic Algorithm Parameters

Parameter	Value
Population size	100
Number of generations	100
Mutation probability	0.20
Crossover rate	0.90

Error Analysis

The average absolute relative deviation (AARD) and total average absolute relative deviation (TAARD) were calculated from the following equations, and the absolute relative deviation (ARD) was considered as the assessment yardstick in vapor pressure calculation,

$$AARD\% = \frac{\sum_{K=1}^{N} \frac{\left|P_{Vpred,K} - P_{V\exp,K}\right|}{P_{V\exp,K}}}{N} \times 100 \quad (23)$$

$$TAARD\% = \frac{\sum AARD,\%}{n} \quad (24)$$

$$ARD\ (in\ fraction)\ \frac{\left|P_{Vpred,K} - P_{V\exp,K}\right|}{P_{V\exp,K}} \quad (25)$$

where P_v is the vapor pressure of DESs, and N is the number of total data points. Subscripts pred and exp represent the predicted vapor pressure from the model and experimental vapor pressure, respectively.

Optimization Process

MATLAB optimization toolbox (Genetic algorithm) was used to achieve a fast, accurate and certain correlation for the k_f factor. Eq. (26) presents the general form of the proposed correlation for the k_f factor,

$$k_f = Ae^{BT+CT_b^2} + \frac{D}{T_b} \quad (26)$$

where A, B, C and D are constants optimized by the Genetic algorithm optimization procedure as shown in Table 4.

RESULTS AND DISCUSSION

The critical properties of DESs were determined using the modified Lydersen-Joback-Reid model. The equations of state (EoSs) were then investigated as a valid strategy for the prediction of vapor pressure. To this end, two different approaches, named φ - φ and γ - φ, were evaluated by several equations of state including Peng-Robinson, Soave-Redlich-Kwong, PR-Twu, Esmaeilzadeh-Roshanfekr as φ - φ approach and the extended NRTL-Ideal, UNIQUAC-Ideal, Wilson-Ideal and CPA-ideal as γ - φ, approach. The results of calculations were summarized in Tables 5 and 6 representing the inefficiency of EoSs in the vapor pressure prediction of DESs. Upon these results, the EoSs have a low accuracy for estimating the vapor pressure of DESs.

The Voutsas model was used as the first technique. The Voutsas model is dependent to the k_f factor (compound specific parameter). k_f is a function of molecular weight and normal boiling point. Figure 2 illustrates the trend of k_f variation with temperature for DESs 1 to 5. This trend expresses a considerable effect of temperature on the k_f factor.

The constants of k_f factor in Eq. (26) were found by Genetic algorithm of MATLAB as 0.7612, 0.0015, -0.000017 and 4.7566 for the pure compounds and 0.0288, 0.0103-0.0000076 and 11.2140 for the aqueous solutions, respectively. Voutsas *et al.* proposed Eq. (14) to calculate the vapor pressure of several classes of organic compounds.

The results obtained from the Modified-Voutsas model for the pure and aqueous solutions of the DESs using the training data set are shown in Figs. 3 and 4, respectively. The deviations of the estimated vapor pressure from the experimental vapor pressure data points are demonstrated in these figures. The Modified-Voutsas model predicted the vapor pressure of pure and aqueous solutions of the DESs within the total average absolute relative deviation range of 7.19 and 9.24% (TAARD%), respectively.

The accuracy of the Modified-Voutsas model for the pure and aqueous solutions of DESs was investigated using the validation data set. Their results are shown in Figs. 5 and 6. The vapor pressures of pure and aqueous solutions of DESs were predicted within the total average absolute relative deviations (TAARD%) of 7.03 and 9.08%, respectively.

Moreover, the Wagner model was described as the second corresponding state model. This model was one of the oldest and the most authentic available models employed in numerous studies. The coefficients of the Wagner model (Eqs. (16)-(18)) were unknown for the heavy compounds such as DESs. So, MATLAB optimization toolbox was employed, and its optimization parameters were obtained. This optimization producer was performed to attain the proper values for the Modified-Wagner model constants. The values of A_1, A_2, A_3, A_4, B_1, B_2, B_3 and B_4 were found to be -6.133, -3.868, 0.673, 3.977, 0.413, 1.552, 3.477, 3.284 and -23.520, 4.633, 25, 12.708, -5.426, 8.629, 2.184, -13.395 for the pure and aqueous solutions of DESs, respectively. An adjustable factor was defined for the Modified-Wagner model by minimizing the summation of the deviations of the predicted vapor pressures from the experimental vapor pressures. This adjusted factor was

Table 5. Vapor Pressure Predicted by the Equations of State (φ - φ Approach)

			Predicted vapor pressure (Pa)							
	Temperature (K)	Vapor pressure (Pa)	PR		SRK		PR-Twu		ER	
			Pred (Pa)[a]	ARD[b]	Pred (Pa)[a]	ARD[a]	Pred (Pa)[a]	ARD[a]	Pred (pa)[a]	ARD[a]
DES-1	343.15	2.1414	38.3	16.9	33.7	14.7	0.0	1.0	0.0	1.0
	353.15	4.3742	76.9	16.6	68.8	14.7	0.0	1.0	0.1	1.0
	363.15	6.8258	147.2	20.6	133.7	18.6	0.0	1.0	0.1	1.0
	373.15	11.6058	270.0	22.3	248.7	20.4	0.0	1.0	0.2	1.0
	383.15	25.4770	476.4	17.7	444.4	16.4	0.1	1.0	2.4	1.0
	393.15	46.1611	790.8	16.2	746.6	15.2	834.8	17.1	796.6	16.3
DES-2	343.15	0.3357	36.7	108.2	32.3	95.1	36.0	106.3	137.9	409.7
	353.15	0.6130	73.9	119.5	66.1	106.9	74.2	120.1	76.6	123.9
	363.15	0.8970	142.1	157.4	129.1	142.9	145.1	160.8	149.1	165.2
	373.15	1.3319	261.6	195.4	241.1	180.0	271.0	202.4	258.8	193.3
	383.15	1.8760	463.1	245.8	432.3	229.4	484.9	257.5	467.7	248.3
	393.15	2.9406	790.8	267.9	746.6	252.9	834.8	282.9	801.5	271.6
DES-3	343.15	2.1578	127.2	57.9	109.6	49.8	0.1	1.0	18.7	7.7
	353.15	5.3127	223.3	41.0	195.6	35.8	0.1	1.0	23.1	3.3
	363.15	9.1210	378.1	40.4	336.3	35.9	0.2	1.0	39.0	3.3
	373.15	16.8544	619.4	35.7	558.4	32.1	0.3	1.0	63.8	2.8
	383.15	32.5043	984.4	29.3	898.7	26.6	0.7	1.0	99.1	2.0
	393.15	60.7790	1521.8	24.0	1405.0	22.1	1.4	1.0	180.3	2.0
DES-4	343.15	0.1379	2276.5	16507.1	2111.7	15312.0	4.2	29.7	217.4	1575.7
	353.15	0.4100	3421.8	8344.8	3206.3	7819.2	8.2	19.0	347.6	846.7
	363.15	0.8501	5014.5	5897.7	4741.8	5576.9	15.3	16.9	513.1	602.6
	373.15	1.7889	7180.2	4012.7	6845.9	3825.9	27.2	14.2	718.4	400.6
	383.15	3.9501	10065.5	2547.2	9668.6	2446.7	46.9	10.9	194.7	48.3
	393.15	6.7878	13838.8	2037.8	13382.5	1970.5	78.2	10.5	137.1	19.2

Table 5. Continued

DES-5	343.15	0.8320	25.9	30.1	21.0	24.3	0.1	0.9	3.5	3.2
	353.15	2.2733	43.9	18.3	36.4	15.0	0.1	0.9	4.5	1.0
	363.15	4.7164	72.3	14.3	60.8	11.9	0.2	0.9	5.1	0.1
	373.15	9.8550	115.5	10.7	98.7	9.0	0.4	1.0	19.1	1.0
	383.15	19.2635	179.6	8.3	155.5	7.1	0.8	0.96	42.5	1.2
	393.15	35.3253	272.4	6.7	238.98	5.8	1.4	0.96	27.6	0.2
TAAR D[c]				1362.3		1277.8		42.2		165.1

[a]Predicted vapor pressure (Pa). [b]Absolute relative deviation (in fraction). [c]Total average absolute relative deviation (in fraction).

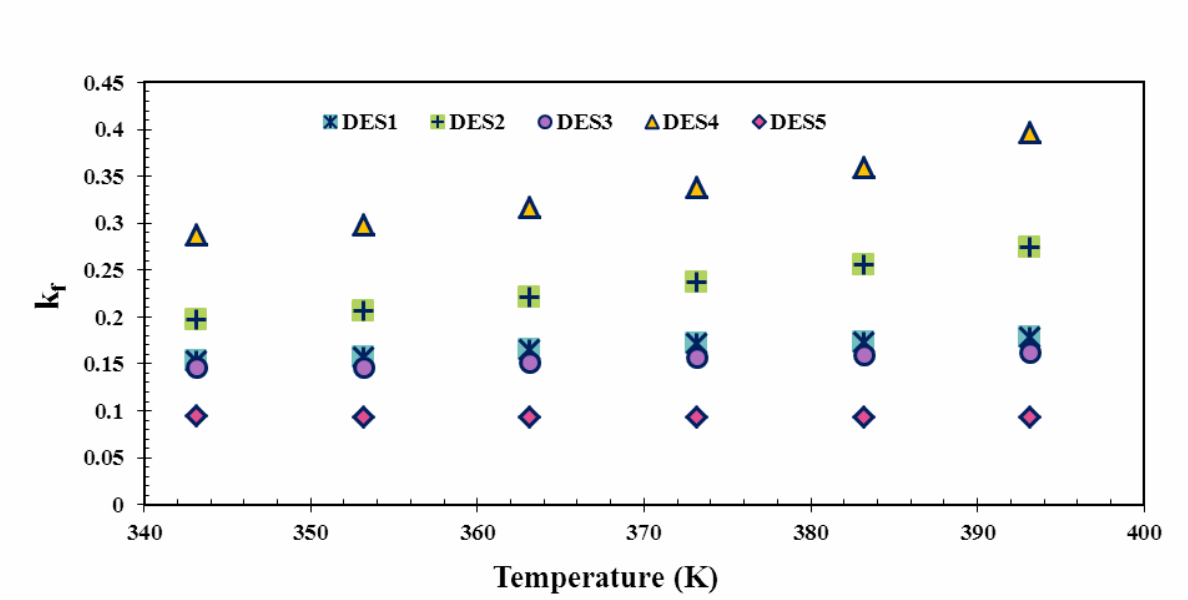

Fig. 2. Effect of temperature on the k_f factor of DESs 1 to 5.

introduced as a function of acentric factor and reduced-temperature. The adjusted factor was described as follows:

$$Adj.Factor = \frac{A + T_r}{B + C\omega} + DT_r \quad (27)$$

where A, B, C and D are constants. MATLAB optimization toolbox was used to estimate these parameters for the pure and aqueous solutions, which were found to be -0.6353, 419.2, -861.82, -0.4184 and -0.3430, -1.2931, 2.0986, -1.2500, respectively. The general form of the Modified-Wagner model is given as follows:

$$\ln P_r^{V} = \ln P_r^{(0)} + \omega \ln P_r^{(1)} + Adj.Factor \quad (28)$$

where $\ln P_r{}^{v}$ means the predicted reduced-vapor pressure. Figures 7 and 8 demonstrate the average absolute relative deviations (AARD%) of the vapor pressure of pure and aqueous solutions of DESs using the Modified-Wagner

Table 6. Vapor Pressure Predicted by the Equations of State (γ - φ Approach)

			Predicted vapor pressure (Pa)					
	Temperature (K)	Vapor pressure (Pa)	Extended NRTL-Ideal		UNIQUAC-Ideal		CPA-Ideal	
			Pred (Pa)[a]	ARD[b]	Pred (Pa)[a]	ARD[b]	Pred (Pa)[a]	ARD[b]
DES-1	343.15	2.1414	98.7	45.1	98.7	45.1	12.6	4.9
	353.15	4.3742	172.4	38.4	171.9	38.3	29.2	5.7
	363.15	6.8258	292.0	41.8	289.9	41.5	63.9	8.4
	373.15	11.6058	480.9	40.4	477.5	40.1	132.6	10.4
	383.15	25.4770	771.6	29.3	771.0	29.3	262.0	9.3
	393.15	46.1611	1186.6	24.7	1181.0	24.6	495.2	9.7
DES-2	343.15	0.3357	95.9	284.5	96.1	285.3	595.0	1771.6
	353.15	0.6130	167.8	272.8	163.3	265.4	1055.2	1720.4
	363.15	0.8970	285.0	316.7	279.6	310.7	1801.5	2007.4
	373.15	1.3319	470.3	352.1	470.1	352.0	2970.8	2229.5
	383.15	1.8760	756.1	402.0	750.8	399.2	4745.8	2528.7
	393.15	2.9406	1186.6	402.5	1181.2	400.7	7364.0	2503.2
DES-3	343.15	2.1578	211.6	97.1	208.2	95.5	1.6	0.2
	353.15	5.3127	343.6	63.7	335.8	62.2	4.1	0.2
	363.15	9.1210	543.2	58.5	544.0	58.6	9.8	0.1
	373.15	16.8544	837.8	48.7	804.4	46.7	22.2	0.3
	383.15	32.5043	1263.5	37.9	1187.1	35.5	47.2	0.4
	393.15	60.7790	1865.9	29.7	1773.5	28.2	95.8	0.6
DES-4	343.15	0.1379	2517.7	18256.1	2343.1	16990.4	429.5	3113.6
	353.15	0.4100	3692.7	9005.5	3002.1	7321.1	772.7	1883.6
	363.15	0.8501	5303.0	6237.1	4956.2	5829.2	1337.0	1571.8
	373.15	1.7889	7469.3	4174.3	6012.5	3360.0	2232.6	1247.0
	383.15	3.9501	10334.1	2615.1	8973.4	2270.7	3608.8	912.6

Table 6. Continued

	393.15	6.7878	14063.4	2070.9	9672.0	1423.9	5661.7	833.1
DES-5	343.15	0.8320	42.5	50.1	30.2	35.3	0.1	0.9
	353.15	2.2733	68.0	28.9	61.6	26.1	0.0	1.0
	363.15	4.7164	106.0	21.5	94.8	19.1	0.0	1.0
	373.15	9.8550	161.4	15.4	157.8	15.0	0.0	1.0
	383.15	19.2635	240.4	11.5	228.2	10.8	0.1	1.0
	393.15	35.3253	350.9	8.9	328.0	8.3	0.2	1.0
TAARD[c]		–		1502.7		1329.0		745.9

[a]Predicted vapor pressure (Pa). [b]Absolute relative deviation (in fraction). [c]Total average absolute relative deviation (in fraction).

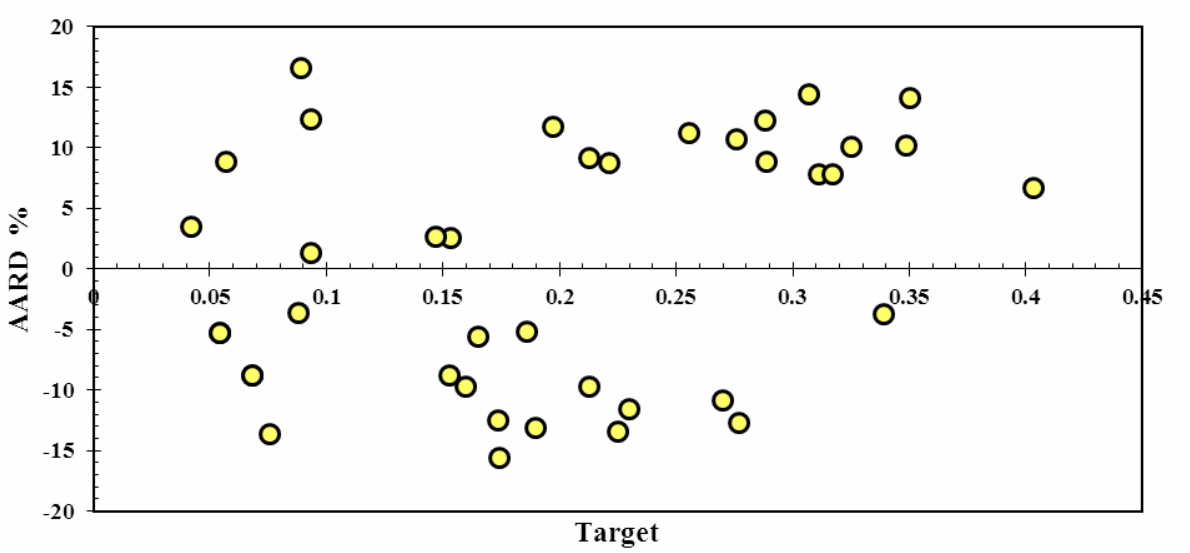

Fig. 3. Deviations of the predicted vapor pressures of the aqueous solutions of the DESs from the experimental values using the Modified-Voutsas model.

model with the help of train data set. The experimental vapor pressure data points expressed the target values.

Results showed that the Modified-Wagner model predicts the vapor pressure of pure and aqueous solutions of the DESs within the total average absolute relative deviation range of 4.98 and 7.21% (TAARD%), respectively. To evaluate the performance of the Modified-Wagner model in estimating the vapor pressure of the pure and aqueous solutions of the DESs, results of the model with the help of validation data set are demonstrated in Figs. 9 and 10. As can be seen, the model is in line with the experimental vapor pressure data, which are not used in obtaining the coefficients of the model. Additionally, the Modified-Wagner model predicted the vapor pressure of pure and

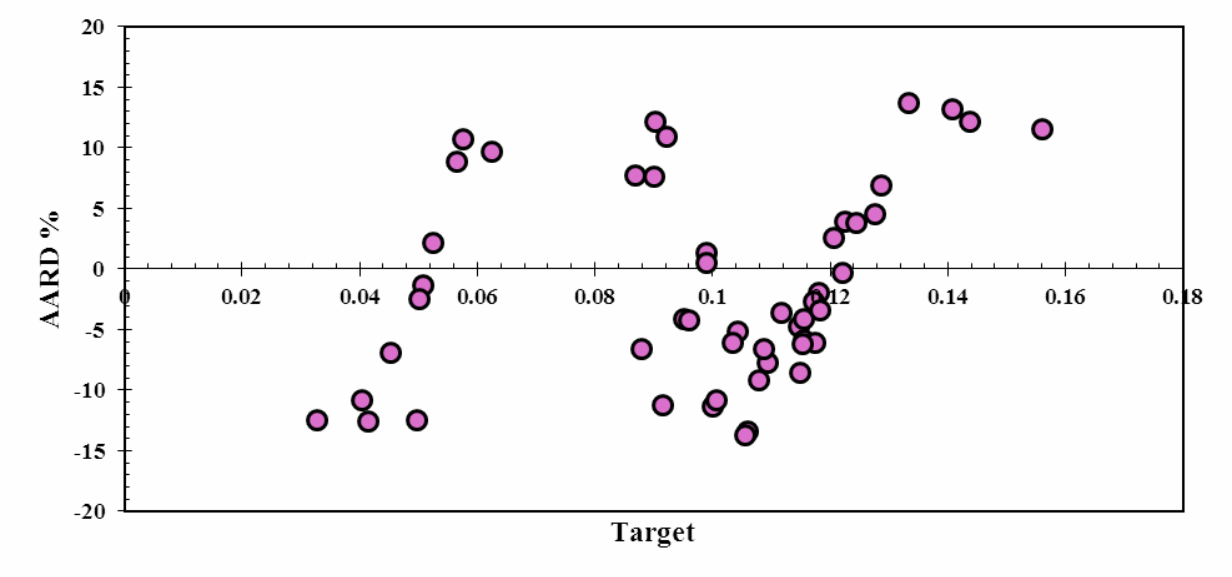

Fig. 4. Deviations of the predicted vapor pressures of pure DESs from the experimental values using the Modified-Voutsas model.

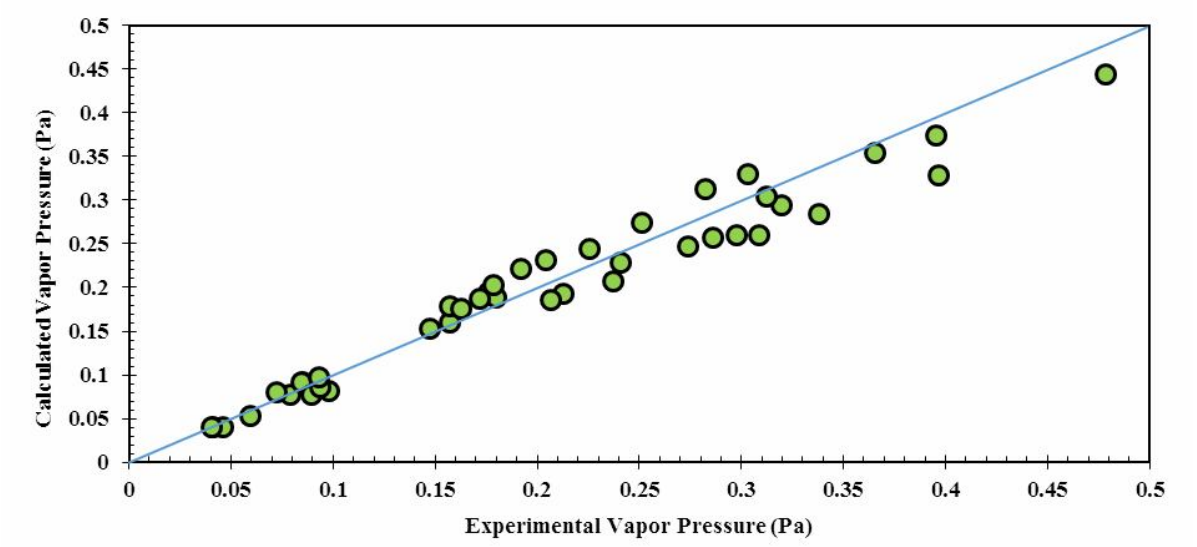

Fig. 5. Validation of the Modified-Voutsas model using the validation data set for the aqueous solutions of DESs.

aqueous solutions of the DESs within the total average error range of 5.47 and 7.15% (TAARD%), respectively.

The average absolute relative deviations (ARRD%) of the EoSs and two mentioned corresponding state models showed that the prediction ability of the DESs vapor pressure using the two mentioned corresponding state models is superior to that of using the investigated EoSs. Additionally, the sensitivity analysis of all the parameters, which are effective and vital in the two modified corresponding states models, was needed to carry out to

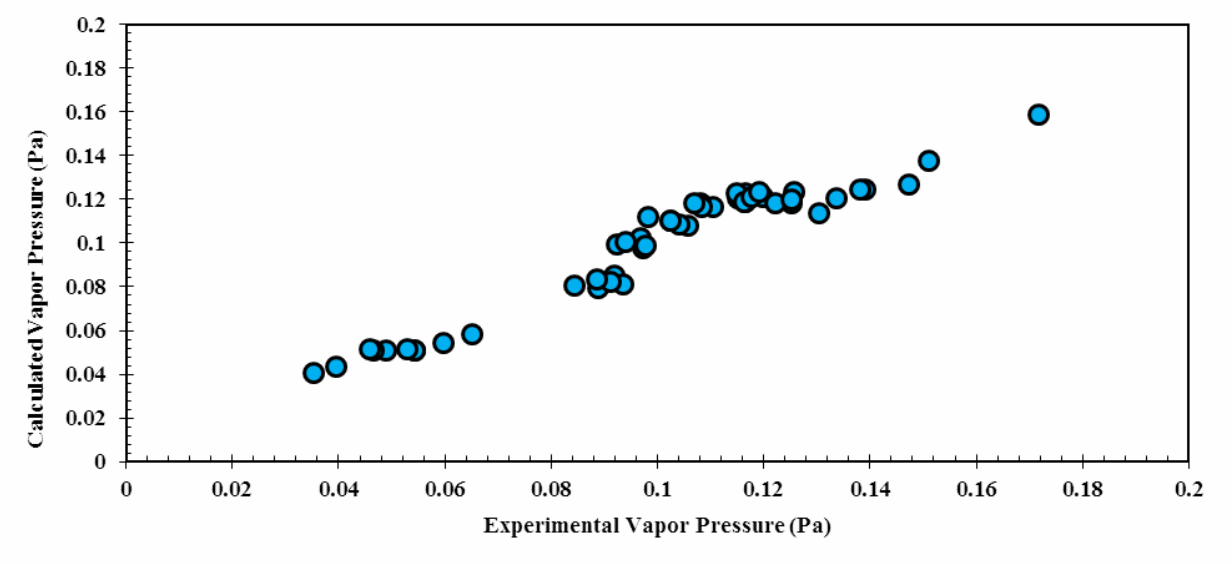

Fig. 6. Validation of the Modified-Voutsas model using the validation data set for the pure DESs.

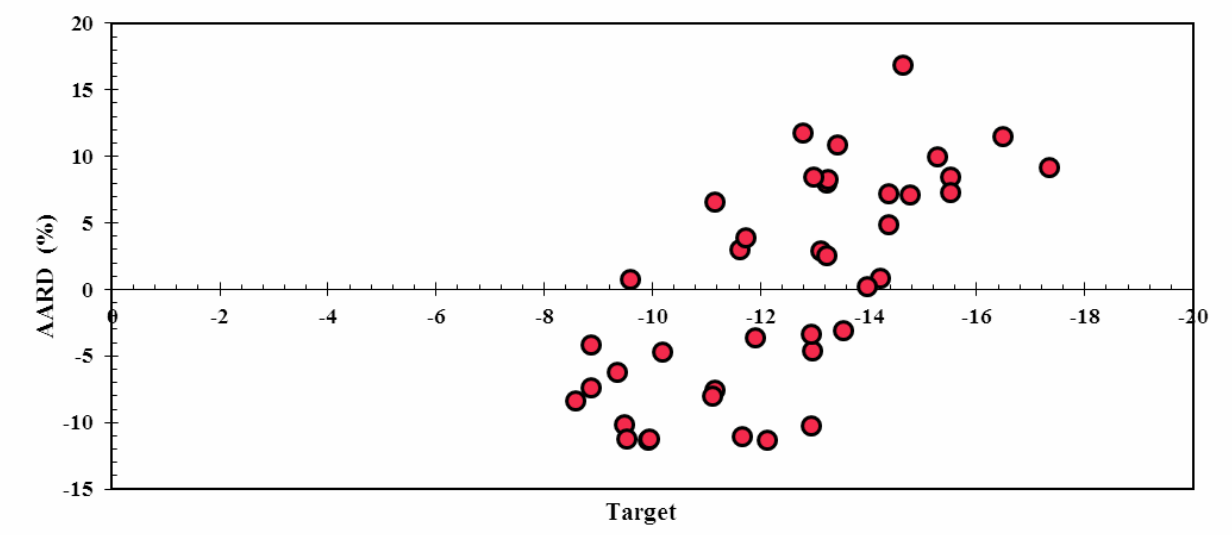

Fig. 7. Deviations of the predicted ln P^v from the experimental data for the aqueous solutions of the DESs using the Modified-Wagner model by the train data set.

obtain the sensitivity of any parameters in the prediction of vapor pressure of DESs. For this purpose, Eq. (29) presenting a correlation for the sensitivity analysis of various models was used. This correlation can be used to investigate the effect of input parameters as the relevancy factors (r) with the range of -1 to +1 [32]. The relevancy factor demonstrated the impact of effective inlet parameters of the two models. The higher relevancy factor represented more effectiveness of this factor in the target values.

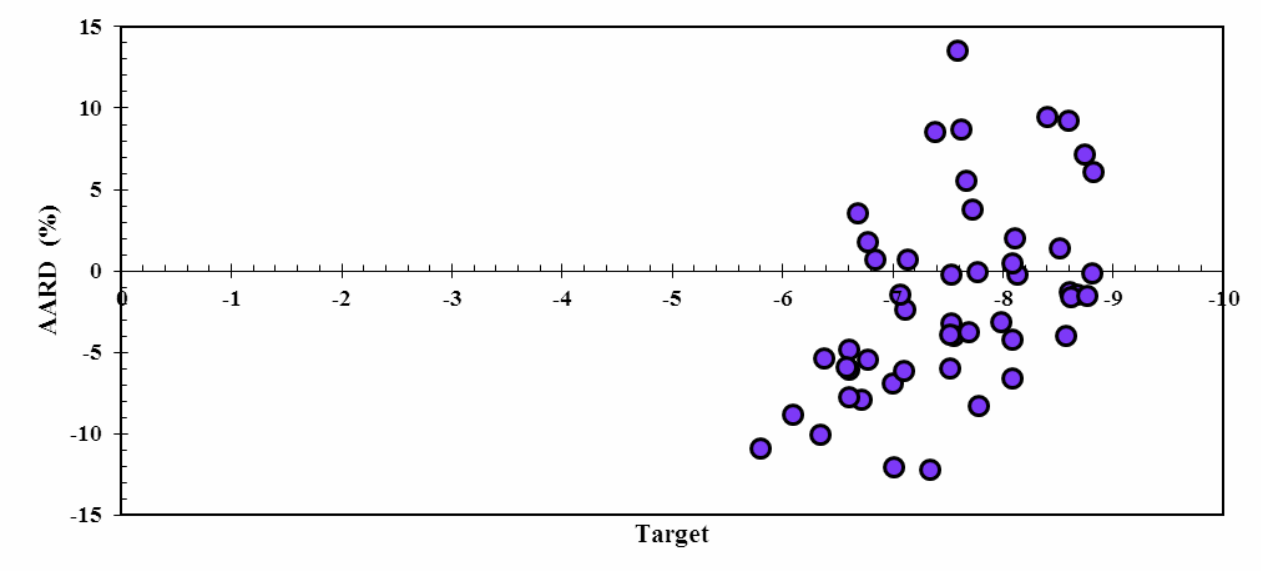

Fig. 8. Deviations of the predicted $\ln P^{v}$ from the experimental data of pure DESs using the Modified-Wagner model by the train data set.

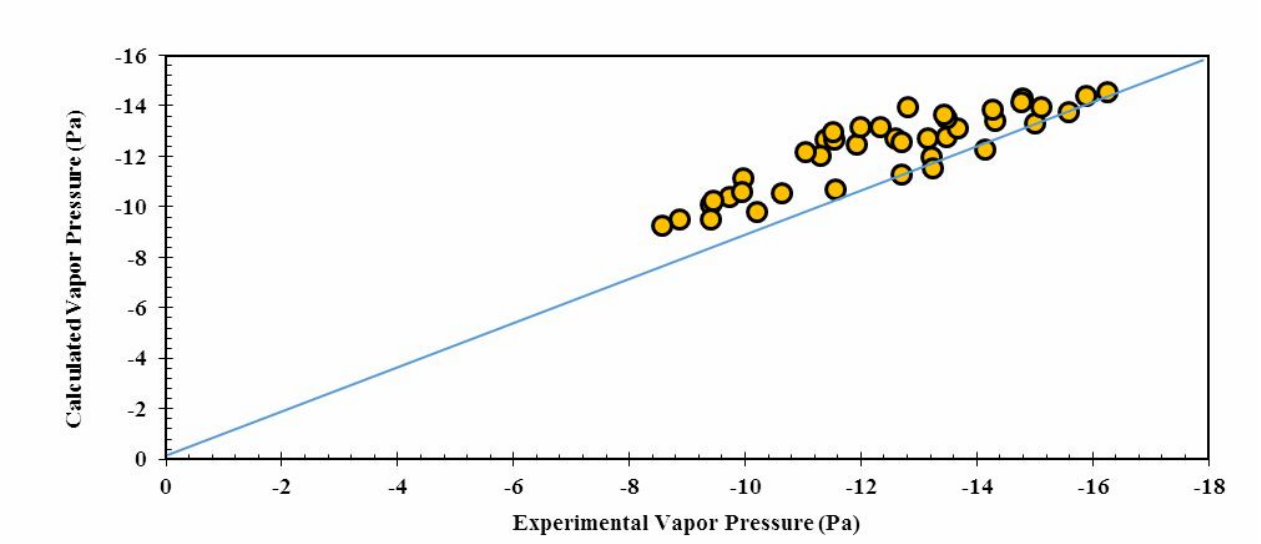

Fig. 9. Validation of the Modified-Wagner model using the validation data set for the aqueous solutions of the DESs.

$$r = \frac{\sum_{i=1}^{N}(X_{k,i} - \overline{X}_k)(y_i - \bar{y})}{\sqrt{\sum_{i=1}^{N}(X_{k,i} - \overline{X}_k)^2 \sum_{i=1}^{N}(y_i - \bar{y})^2}} \quad (29)$$

where $X_{k,i}$, $\overline{X}_k$, y_i, $\bar{y}$ and N denote the input value, average input value, output value, average output value and the total number of data points, respectively.

Figures 11 and 12 demonstrate the results obtained from the sensitivity analysis of the Modified-Voutsas and Modified-Wagner models, respectively. The acentric factor, normal boiling point and temperature were the input parameters of the Modified-Voutsas model. According to Fig. 11, temperature is an efficient input factor due to the high relevancy factor. The acentric factor and normal

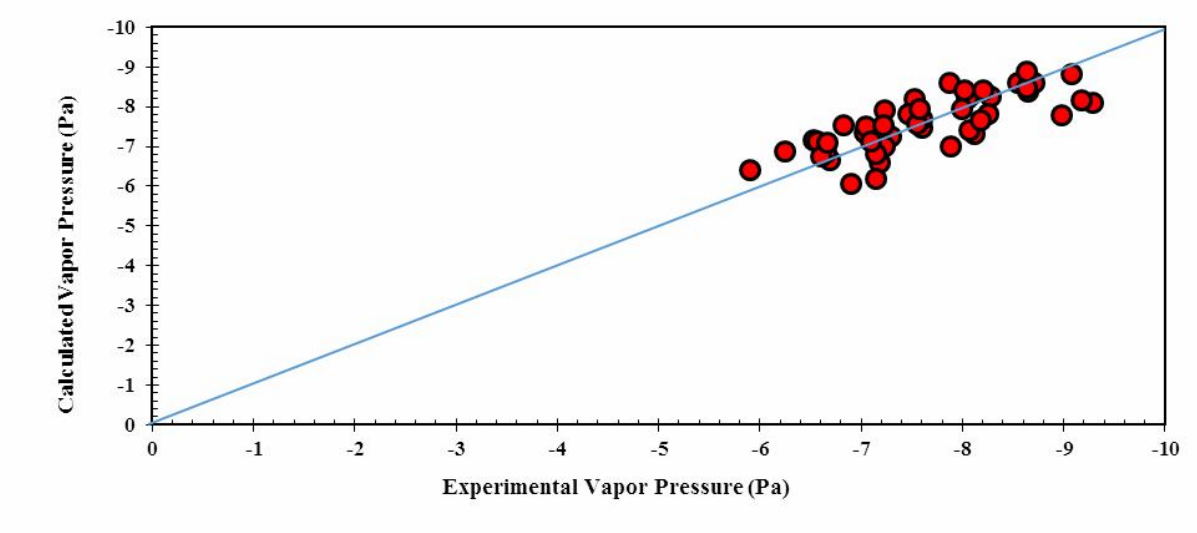

Fig. 10. Validation of the Modified-Wagner model using the validation data set for the pure DESs.

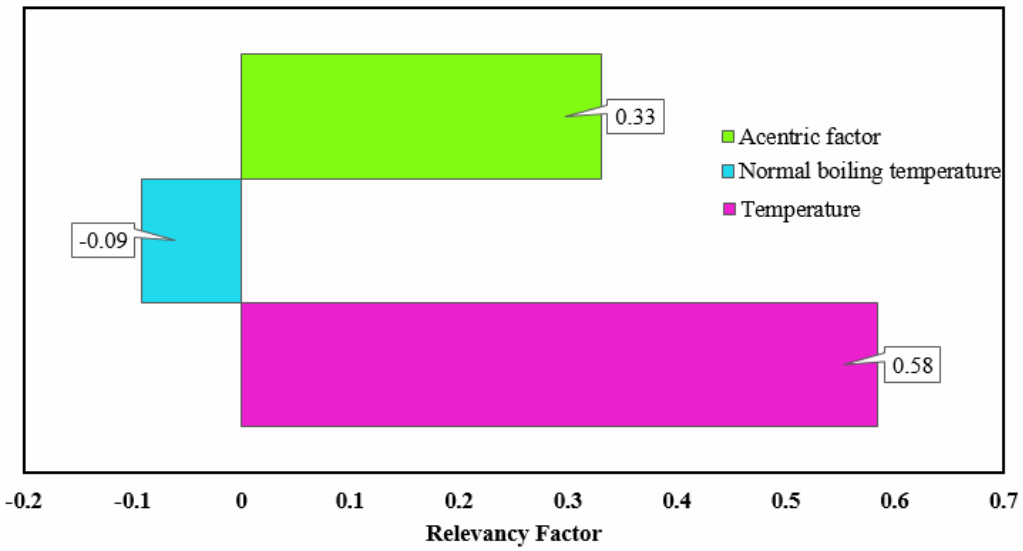

Fig. 11. Sensitivity analysis of the Modified-Voutsas model.

boiling point were the other efficient parameters, in sequence. Additionally, the sensitivity analysis of the Modified-Wagner model was done with the input parameters including the critical temperature, critical pressure, acentric factor and temperature, as shown in Fig. 12. Moreover, the relevancy factor of all the input parameters is illustrated in Fig. 12. The results obtained from Fig. 12 demonstrate the significant effect of critical pressure on the relevancy factor as compared to the other ones. The critical temperature, acentric factor and temperature have almost the same impact on the relevancy factor.

In order to evaluate the validity of the DESs vapor pressure calculations by the Modified-Voutsas and Modified-Wagner models, the specific heat capacity of DES-2 and DES-12 to DES-35 (476 data points) was

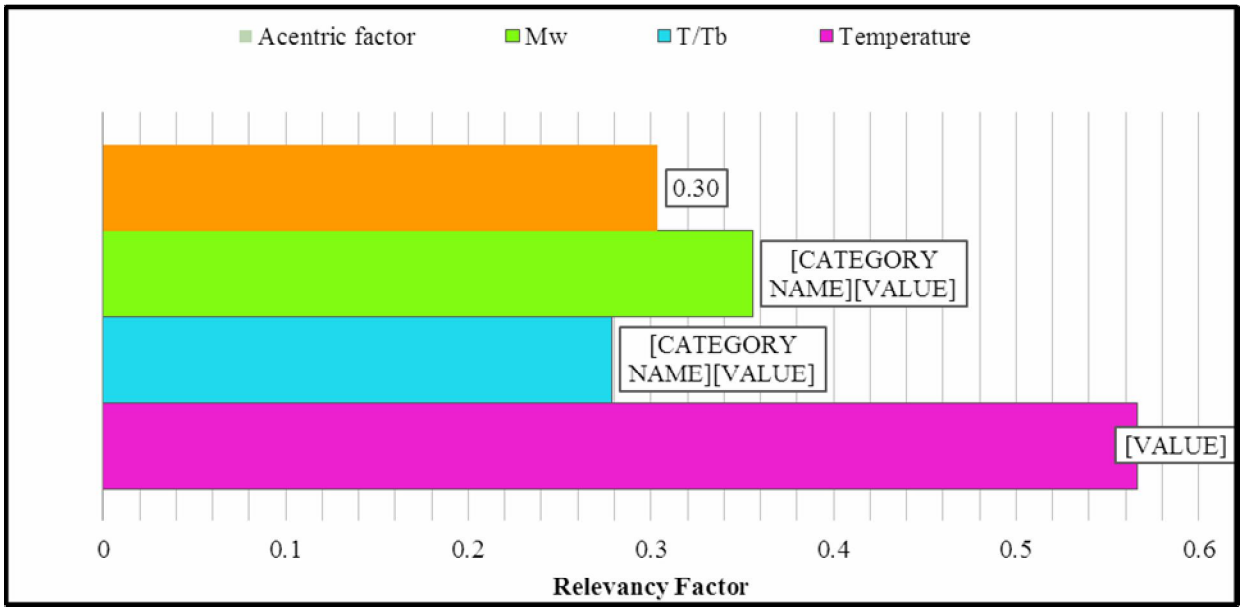

Fig. 12. Sensitivity analysis of the Modified-Wagner model.

Table 7. Specific Heat Capacity Predicted by the Modified Voutsas and Wagner Models

DES	Temperature range (K)	Number of data points	Experimental average of specific heat capacity, Cp ($J\ mol^{-1}\ K^{-1}$)	Modified Voutsas model	AARD (%)[a]	Modified Wagner model	AARD (%)[a]
DES-12	278.15-295.65	8	166.16	171.48	3.20	157.85	5.00
DES-12	298.15-338.15	17	171.94	170.04	1.11	179.69	4.51
DES-14	278.15-298.15	11	159.81	159.74	0.05	161.52	1.07
DES-14	305.65-325.65	14	166.61	165.84	0.46	166.47	0.08
DES-15	300-330	7	134.43	133.30	0.84	146.22	8.78
DES-16	298.15-303.15	3	300.26	299.96	0.10	308.51	2.74
DES-17	298.15-310.65	6	228.54	224.13	1.93	244.28	6.89
DES-17	313.15-330.65	8	232.48	218.35	6.08	242.47	4.30
DES-17	333.15-335.65	9	238.15	259.87	9.12	230.72	3.12
DES-18	298.15-305.65	4	271.85	249.61	8.18	244.40	10.10
DES-18	308.15-315.65	4	274.98	292.93	6.53	285.11	3.69
DES-18	325.65-335.65	5	278.35	274.93	1.23	281.54	1.15

Table 7. Continued

DES-19	298.15-310.65	6	221.76	237.08	6.91	214.51	3.27
DES-19	313.15-328.15	7	227.21	230.79	1.57	218.80	3.70
DES-19	330.65-353.15	10	233.29	227.19	2.62	220.86	5.33
DES-20	298.15-305.65	4	290.28	308.60	6.31	307.39	5.90
DES-20	308.15-318.15	5	295.64	279.83	5.35	319.39	8.03
DES-20	320.65-333.15	6	301.97	286.06	5.27	311.04	3.00
DES21	298.15-305.65	4	239.10	216.54	9.44	254.51	6.45
DES-21	330.65-343.15	15	252.15	236.10	6.37	252.23	0.03
DES-22	298.15-308.15	5	229.79	229.48	0.14	236.06	2.73
DES-22	308.15-315.65	4	233.84	230.11	1.60	226.20	3.27
DES-22	318.15-325.65	4	237.91	231.16	2.83	247.49	4.03
DES-22	328.15-335.65	4	241.69	232.64	3.75	229.01	5.25
DES-23	298.15-313.15	7	190.19	186.83	1.77	176.40	7.25
DES-23	315.65-330.65	7	196.37	191.05	2.71	181.98	7.33
DES-23	333.15-353.15	9	202.41	196.30	3.02	186.43	7.90
DES-24	298.15-320.65	10	137.80	138.84	0.75	134.98	2.05
DES-24	323.15-353.15	13	144.36	144.46	0.06	139.58	3.31
DES-25	298.15-315.65	8	94.11	88.45	6.01	96.16	2.18
DES-25	381.15-338.15	9	96.24	88.93	7.59	98.09	1.92
DES-26	298.15-303.15	3	365.47	401.71	9.91	400.15	9.49
DES-26	305.65-310.65	3	369.56	403.22	9.11	405.32	9.68
DES-26	313.15-318.15	3	373.86	405.16	8.37	409.67	9.58
DES-26	320.65-325.65	3	378.05	407.52	7.80	412.97	9.24
DES-26	328.15-333.15	3	382.19	410.28	7.35	416.64	9.01
DES-26	335.65-340.65	3	385.66	413.43	7.20	417.15	8.17
DES-26	343.15-353.15	5	391.38	416.96	6.54	420.54	7.45
DES-27	298.15-310.65	6	274.72	295.82	7.68	245.85	10.51
DES-27	313.15-325.65	6	281.00	303.90	8.15	307.50	9.43
DES-27	328.15-353.15	11	289.49	261.75	9.58	310.33	7.20
DES-28	298.15-320.65	10	191.62	194.17	1.33	185.97	2.95

Table 7. Continued

DES-28	323.15-353.15	13	199.81	205.60	2.90	207.66	3.93
DES-29	298.15-315.65	8	126.29	129.47	2.52	130.23	3.12
DES-29	318.15-353.15	15	130.46	131.89	1.10	134.10	2.79
DES-30	298.15-305.65	4	290.29	308.60	6.31	273.26	5.87
DES-30	298.15-318.15	5	295.63	279.83	5.34	271.97	8.00
DES-30	320.65-333.15	6	301.98	286.06	5.27	292.88	3.01
DES-30	335.65-353.15	8	308.88	321.99	4.24	298.41	3.39
DES-31	298.15-303.15	3	245.32	270.76	10.37	250.83	2.25
DES-31	305.65-310.65	3	248.83	275.31	10.64	254.11	2.12
DES-31	313.15-318.15	3	251.97	275.26	9.24	258.17	2.46
DES-31	320.65-325.65	3	255.35	275.51	7.90	261.09	2.25
DES-31	328.15-333.15	3	257.57	276.03	7.17	253.46	1.60
DES-31	335.65-340.65	3	261.68	276.83	5.79	265.85	1.59
DES-31	343.15-345.65	3	264.41	277.88	5.10	261.74	1.01
DES-31	348.15-353.15	3	266.68	266.89	0.08	263.81	1.08
DES-32	298.15-310.65	6	215.25	219.85	2.14	208.18	3.28
DES-32	313.15-326.65	6	221.15	223.84	1.22	211.51	4.36
DES-32	328.15-350.65	11	228.46	228.74	0.12	213.86	6.39
DES-33	298.15-320.65	10	179.51	171.70	4.35	184.06	2.54
DES-33	323.15-353.15	13	188.82	180.57	4.37	187.29	0.81
DES-34	298.15-325.65	12	137.61	139.08	1.07	139.90	1.66
DES-34	328.15-353.15	11	144.43	143.07	0.94	147.24	1.94
DES-35	298.15-315.65	8	98.69	92.92	5.84	95.22	3.52
DES-35	318.15-335.65	8	100.18	93.58	6.59	96.25	3.93
DES-35	338.15-353.15	7	101.58	104.92	3.29	97.56	3.96
DES-2	305-335	7	194.78	184.95	5.05	188.52	3.22
DES-2	340-355	4	202.76	209.87	3.51	204.29	0.76
DES-2	305-325	5	182.76	202.16	10.62	179.08	2.01
DES-2	330-355	6	187.90	169.93	9.57	180.00	4.21
Total	278.15-353.15	476	94.11-391.38	88.45-416.96	4.77^{**}	95.22-420.54	4.42^{**}

[a]Average absolute relative deviation. [b]TAARD (%).

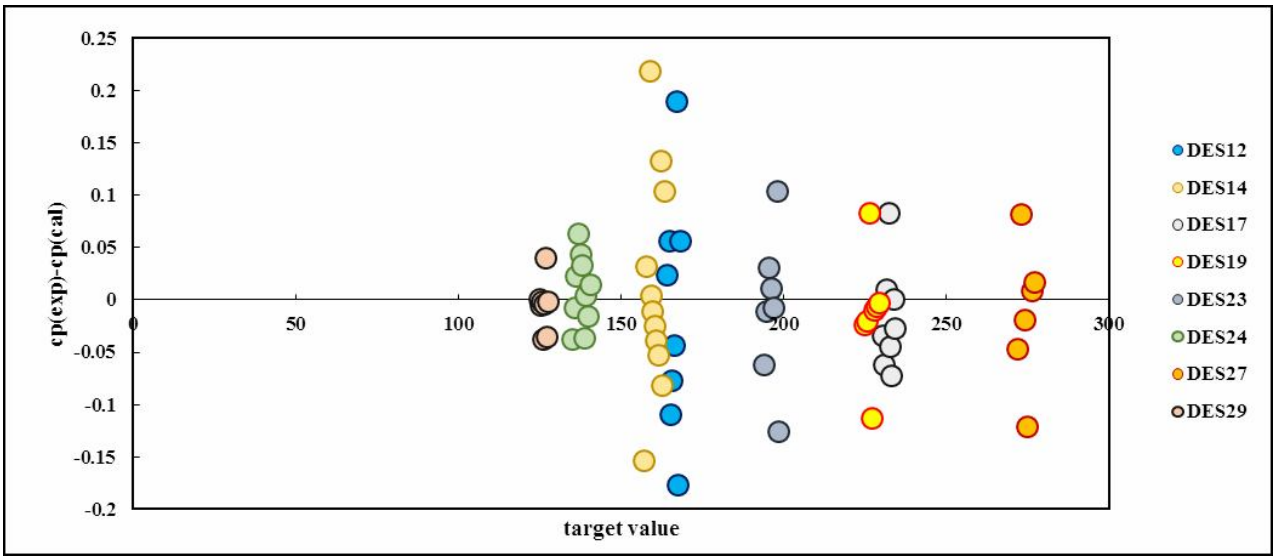

Fig. 13. Deviations of the predicted specific heat capacities from the experimental data points for the pure and aqueous solutions of the DESs using the linear equation and the train data set.

Table 8. Predicted Values of the Average Specific Heat Capacity Using the Linear Equation

DES	Temperature range	Number of data points	a	*b*	Cp_{avg} ($J\ mol^{-1}\ K^{-1}$)	AARD (%)
DES-12	278.15-295.65	8	0.23	101.12	166.16	0.06
DES-12	298.15-338.15	17	0.23	99.49	171.94	0.05
DES-14	278.15-298.15	11	0.25	89.01	159.81	0.05
DES-14	305.65-325.65	14	0.25	88.74	166.61	0.05
DES-15	300-330	7	0.10	101.98	134.43	0.26
DES-16	298.15-303.15	3	0.50	149.94	300.26	0.01
DES-17	298.15-310.65	6	0.26	150.61	228.54	0.03
DES-17	313.15-330.65	8	0.21	164.56	232.48	0.02
DES-17	333.15-335.65	9	0.28	142.51	238.15	0.11
DES-18	298.15-305.65	4	0.24	199.39	271.85	0.05
DES-18	308.15-315.65	4	0.36	163.94	274.98	0.01
DES-18	325.65-335.65	5	0.21	208.25	278.35	0.17
DES-19	298.15-310.65	6	0.40	101.40	221.76	0.02

Table 8. Continued

DES-19	313.15-328.15	7	0.28	137.88	227.21	0.02
DES-19	330.65-353.15	10	0.26	146.11	233.29	0.11
DES-20	298.15-305.65	4	0.52	132.08	290.28	0.01
DES-20	308.15-318.15	5	0.47	149.09	295.64	0.03
DES-20	320.65-333.15	6	0.42	164.87	301.97	0.05
DES21	298.15-305.65	4	0.42	113.51	239.10	0.05
DES-21	330.65-343.15	15	0.36	130.87	252.15	0.29
DES-22	298.15-308.15	5	0.39	111.45	229.79	0.01
DES-22	308.15-315.65	4	0.41	104.96	233.84	0.01
DES-22	318.15-325.65	4	0.38	116.36	237.91	0.01
DES-22	328.15-335.65	4	0.38	115.17	241.69	0.05
DES-23	298.15-313.15	7	0.35	84.62	190.19	0.04
DES-23	315.65-330.65	7	0.32	93.09	196.37	0.03
DES-23	333.15-353.15	9	0.28	105.61	202.41	0.12
DES-24	298.15-320.65	10	0.24	62.34	137.80	0.02
DES-24	323.15-353.15	13	0.20	75.31	144.36	0.08
DES-25	298.15-315.65	8	0.11	61.52	94.11	0.03
DES-25	381.15-338.15	9	0.09	66.41	96.24	0.03
DES-26	298.15-303.15	3	0.56	197.71	365.47	0.02
DES-26	305.65-310.65	3	0.59	187.75	369.56	0.01
DES-26	313.15-318.15	3	0.59	187.63	373.86	0.01
DES-26	320.65-325.65	3	0.47	227.46	378.05	0.01
DES-26	328.15-333.15	3	0.56	197.69	382.19	0.01
DES-26	335.65-340.65	3	0.59	186.15	385.66	0.01
DES-26	343.15-353.15	5	0.53	205.33	391.38	0.01
DES-27	298.15-310.65	6	0.41	149.15	274.72	0.02
DES-27	313.15-325.65	6	0.41	149.41	281.00	0.03
DES-27	328.15-353.15	11	0.40	153.81	289.49	0.06
DES-28	298.15-320.65	10	0.27	107.12	191.62	0.10
DES-28	323.15-353.15	13	0.26	113.28	199.81	0.08

Table 8. Continued

DES-29	298.15-315.65	8	0.15	80.13	126.29	0.01
DES-29	318.15-353.15	15	0.13	86.09	130.46	0.06
DES-30	298.15-305.65	4	0.52	134.75	290.29	0.01
DES-30	298.15-318.15	5	0.46	150.08	295.63	0.02
DES-30	320.65-333.15	6	0.42	164.06	301.98	0.05
DES-30	335.65-353.15	8	0.34	191.13	308.88	0.09
DES-31	298.15-303.15	3	0.45	110.63	245.32	0.01
DES-31	305.65-310.65	3	0.49	97.83	248.83	0.01
DES-31	313.15-318.15	3	0.40	124.45	251.97	0.01
DES-31	320.65-325.65	3	0.42	118.33	255.35	0.01
DES-31	328.15-333.15	3	0.19	194.75	257.57	0.01
DES-31	335.65-340.65	3	0.40	125.07	261.68	0.01
DES-31	343.15-345.65	3	0.42	118.38	264.41	0.01
DES-31	348.15-353.15	3	0.53	80.13	266.68	0.01
DES-32	298.15-310.65	6	0.41	91.11	215.25	0.02
DES-32	313.15-326.65	6	0.39	96.78	221.15	0.03
DES-32	328.15-350.65	11	0.35	110.18	228.46	0.08
DES-33	298.15-320.65	10	0.34	74.25	179.51	0.03
DES-33	323.15-353.15	13	0.32	80.68	188.82	0.08
DES-34	298.15-325.65	12	0.25	59.88	137.61	0.03
DES-34	328.15-353.15	11	0.23	66.56	144.43	0.06
DES-35	298.15-315.65	8	0.08	73.95	98.69	0.01
DES-35	318.15-335.65	8	0.08	75.14	100.18	0.05
DES-35	338.15-353.15	7	0.09	72.17	101.58	0.05
DES-2	305-335	7	0.27	108.32	194.78	0.04
DES-2	340-355	4	0.32	91.56	202.76	0.02
DES-2	305-325	5	0.15	136.01	182.76	0.09
DES-2	330-355	6	0.21	114.78	187.90	0.06
Total	278.15-353.15	476	0.08-0.59	59.88-227.46	94.11-391.38	0.04[a]

[a]TAARD (%).

predicted using the vapor pressure data obtained from the modified models and then their results were compared with the experimental data reported in the literature [19,32-35].

Table 8 demonstrates the average absolute relative deviations between the experimental and predicted values of the specific heat capacity of different classes of DESs studied in this investigation. As can be seen, a good prediction for the specific heat capacity of DESs in the temperature range of 278.15-353.15 K has been achieved. The specific heat capacities of different classes of DESs were predicted using the Modified-Wagner and Modified-Voutsas models with a total average absolute relative deviation of 4.42 and 4.77%, respectively.

The general form of a linear equation is given as follows:

$$C_p = aT + b \tag{30}$$

where C_P means the predicted specific heat capacity and a and b are constants, which are dependent to the temperature. Table 8 and Fig. 13 demonstrate the average absolute relative deviation (AARD%) of the specific heat capacity of pure and aqueous solutions of DESs using the linear equation using the train data set. The target values shown in Fig.13 stand the experimental specific heat capacity of the data points.

CONCLUSIONS

12 DESs made from 5 salts and 7 hydrogen bond donors (HBDs) with different combinations of molar ratio (81 experimental data set of 9 pure compounds and 100 experimental data set of 4 aqueous solutions) were used to determine their vapor pressures *via* two modified corresponding state models within the temperature range of 343-393 K. The results of two various models (Modified-Voutsas and Modified-Wagner models) using the corresponding state theory demonstrated that this strategy is appropriate for the prediction of DESs vapor pressure with a TAARD less than 9.5%. In other words, the Modified-Voutsas and Modified-Wagner models were efficient methods for the prediction of vapor pressure of various types of DESs with different salts and HBDs with higher accuracy as compared to the EoSs including the ER, PR, SRK, PR-Twu, Extended NRTL-Ideal, UNIQUAC-Ideal, CPA-Ideal and the GC-VW equations, as well as two corresponding-state models including the Voutsas and Wagner models. In order to confirm the accuracy of the vapor pressure calculations by the Modified-Voutsas and Modified-Wagner models, the average specific heat capacity of the DESs was estimated with the vapor pressure data obtained from these models and was compared with the experimental data. Results show that the vapor pressure calculation by the modified proposed models treats different classes of DESs in specific heat capacity calculation with an acceptable accuracy.

ACKNOWLEDGEMENTS

The authors would like to express their appreciation to the Shiraz University and Sultan Qaboos University.

REFERENCES

[1] De María, P. D.; Maugeri, Z., Ionic liquids in biotransformations: From proof-of-concept to emerging deep-eutectic-solvents, *Curr. Opin. Chem. Biol.,* **2011**, *15*, 220-225, DOI: 10.1016/j.cbpa.2010.11.008.

[2] Abbott, A. P.; Boothby, D.; Capper, G.; Davies, D. L.; Rasheed, R. K., Deep eutectic solvents formed between choline chloride and carboxylic acids: Versatile alternatives to ionic liquids, *J. Am. Chem. Soc.,* **2004**, *126*, 9142-9147, DOI: 10.1021/ja048266j.

[3] Bi, W.; Tian, M.; Row, K. H., Evaluation of alcohol-based deep eutectic solvent in extraction and determination of flavonoids with response surface methodology optimization, *J. Chromatogr. A.,* **2013**, *1285*, 22-30, DOI: 10.1016/j.chroma.2013.02.041.

[4] Leron, R. B.; Caparanga, A.; Li, M. H., Carbon dioxide solubility in a deep eutectic solvent based on choline chloride and urea at T = 303.15-343.15 K and moderate pressures, *J. Taiwan Inst. Chem. Eng.,* **2013**, *44*, 879-885, DOI: 10.1016/j.jtice.2013.02.005.

[5] Liao, H. G.; Jiang, Y. X.; Zhou, Z. Y.; Chen, S. P.; Sun, S. G., Shape-controlled synthesis of gold

nanoparticles in deep eutectic solvents for studies of structure-functionality relationships in electrocatalysis, *Angew. Chem. Int. Ed.,* **2008**, *47*, 9100-9103, DOI: 10.1002/anie.200803202.

[6] Paiva, A.; Craveiro, R.; Aroso, I.; Martins, M.; Reis, R. L.; Duarte, A. R. C., Natural deep eutectic solvents–solvents for the 21st century, *ACS Sustain. Chem. Eng.,* **2014**, *2*, 1063-1071, DOI: 10.1021/sc500096j.

[7] Troter, D. Z.; Todorović, Z. B.; Đokić-Stojanović, D. R.; Stamenković, O. S.; Veljković, V. B., Application of ionic liquids and deep eutectic solvents in biodiesel production: A review, *Renew. Sust. Energ. Rev.,* **2016**, *61*, 473-500, DOI: 10.1016/j.rser.2016.04.011.

[8] Atilhan, M.; Costa, L. T.; Aparicio, S., Elucidating the properties of graphene-deep eutectic solvents interface, *Langmuir,* **2017**, *33*, 5154-5165, DOI: 10.1021/acs.langmuir.7b00767.

[9] Smith, E. L.; Abbott, A. P.; Ryder, K. S., Deep eutectic solvents (DESs) and their applications, *Chem. Rev.,* **2014**, *114*, 11060-11082, DOI: 10.1021/cr300162p.

[10] Tang, B.; Row, K. H., Recent developments in deep eutectic solvents in chemical sciences, *Monatsh. Chem.,* **2013**, *144*, 1427-1454, DOI: 10.1007/s00706-013-1050-3.

[11] Schwarzenbach, R. P.; Gschwend P. M., Environmental Organic Chemistry, John Wiley & Sons, 2016.

[12] Goodarzi, M.; Dos Santos Coelho, L.; Honarparvar, B.; Ortiz, E. V.; Duchowicz, P. R., Application of quantitative structure-property relationship analysis to estimate the vapor pressure of pesticides, *Ecotoxicol. Environ. Saf.,* **2016**, *128*, 52-60, DOI: 10.1016/j.ecoenv.2016.01.020.

[13] Kousksou, T.; Bruel, P.; Jamil, A.; El Rhafiki, T.; Zeraouli, Y., Energy storage: Applications and challenges, *Sol. Energy Mater. Sol. Cells,* **2014**, *120*, 59-80, DOI: 10.1016/j.solmat.2013.08.015.

[14] Kolb, C. E.; Worsnop, D. R., Chemistry and composition of atmospheric aerosol particles, *Annu. Rev. Phys. Chem.,* **2012**, *63*, 471-491, DOI: 10.1146/annurev-physchem-032511-143706.

[15] Gharagheizi, F.; Eslamimanesh, A.; Ilani-Kashkouli, P.; Mohammadi, A. H.; Richon, D., QSPR molecular approach for representation/prediction of very large vapor pressure dataset, *Chem. Eng. Sci.,* **2012**, *76*, 99-107, DOI: 10.1016/j.ces.2012.03.033.

[16] Ma, W.; Zhang, L.; Yang, C., Discussion of the applicability of the generalized Clausius-Clapeyron equation and the frozen fringe process, *Earth Sci. Rev.,* **2015**, *142*, 47-59, DOI: 10.1016/j.earscirev.2015.01.003.

[17] Shahbaz, K.; Mjalli, F. S.; Vakili-Nezhaad, G.; AlNashef, I. M.; Asadov, A.; Farid, M. M., Thermogravimetric measurement of deep eutectic solvents vapor pressure, *J. Mol. Liq.,* **2016**, *222*, 61-66, DOI: 10.1016/j.molliq.2016.06.106.

[18] Dietz, C. H.; Creemers, J. T.; Meuleman, M. A.; Held, C.; Sadowski, G.; Van Sint Annaland, M.; Gallucci, F.; Kroon, M. C., Determination of the total vapor pressure of hydrophobic deep eutectic solvents: Experiments and PC-SAFT modelling, *ACS Sustain. Chem. Eng.,* **2019**, *7*, 4047-4057, DOI: 10.1021/acssuschemeng.8b05449.

[19] Ma, C.; Guo, Y.; Li, D.; Zong, J.; Ji, X.; Liu, C.; Lu, X., Molar enthalpy of mixing for choline chloride/urea deep eutectic solvent + water system, *J. Chem. Eng. Data,* **2016**, *61*, 4172-4177, DOI: 10.1021/acs.jced.6b00569.

[20] Ma, C.; Guo, Y.; Li, D.; Zong, J.; Ji, X.; Liu, C., Molar enthalpy of mixing and refractive indices of choline chloride-based deep eutectic solvents with water, *J. Chem. Thermodyn.,* **2017**, *105*, 30-36, DOI: 10.1016/j.jct.2016.10.002.

[21] Wu, S. H.; Caparanga, A. R.; Leron, R. B.; Li, M. H., Vapor pressure of aqueous choline chloride-based deep eutectic solvents (ethaline, glyceline, maline and reline) at 30-70 C, *Thermochim. Acta,* **2012**, *544*, 1-5, DOI: 10.1016/j.tca.2012.05.031.

[22] Shahbaz, K.; Mjalli, F. S.; Hashim, M. A.; AlNashef, I. M., Prediction of deep eutectic solvents densities at different temperatures, *Thermochim. Acta,* **2011**, *515*, 67-72, DOI: 10.1016/j.tca.2010.12.022.

[23] Valderrama, J. O.; Rojas, R. E., Critical properties of ionic liquids, *Ind. Eng. Chem. Res.,* **2009**, *48*, 6890-

6900, DOI: 10.1021/ie900250g.

[24] Veny, H.; Baroutian, S.; Aroua, M. K.; Hasan, M.; Raman, A. A.; Sulaiman, N. M. N., Density of Jatropha curcas seed oil and its methyl esters: Measurement and estimations, *Int. J. Thermophy,* **2009**, *30*, 529-541, DOI: 10.1007/s10765-009-0569-3.

[25] Li, C.; Jia, W.; Wu, X., Temperature prediction for high pressure high temperature condensate gas flow through chokes, *Energies,* **2012**, *5*, 670-682, DOI: 10.3390/en5030670.

[26] Panteli, E.; Voutsas, E.; Magoulas, K.; Tassios, D., Prediction of vapor pressures and enthalpies of vaporization of organic compounds from the normal boiling point temperature, *Fluid Phase Equilib.,* **2006**, *248*, 70-77, DOI: 10.1016/j.fluid.2006.07.008.

[27] Twu, C. H.; Coon, J. E.; Cunningham, J. R., A generalized vapor pressure equation for heavy hydrocarbons, *Fluid Phase Equilib.,* **1994**, *96*, 19-31, DOI: 10.1016/0378-3812(94)80085-5.

[28] Lapeña, D.; Lomba, L.; Artal, M.; Lafuente, C.; Giner, B., Thermophysical characterization of the deep eutectic solvent choline chloride: Ethylene glycol and one of its mixtures with water, *Fluid Phase Equilib.,* **2019**, *492*, 1-9, DOI: 10.1016/j.fluid.2019.03.018.

[29] Castro, V. I.; Mano, F.; Reis, R. L.; Paiva, A.; Duarte, A. R. C., Synthesis and physical and thermodynamic properties of lactic acid and malic acid-based natural deep eutectic solvents, *J. Chem. Eng. Data,* **2018**, *63*, 2548-2556, DOI: 10.1021/acs.jced.7b01037.

[30] Naser, J.; Mjalli, F. S.; Gano, Z. S., Molar heat capacity of selected type III deep eutectic solvents, *J. Chem. Eng. Data,* **2016**, *61*, 1608-1615, DOI: 10.1021/acs.jced.5b00989.

[31] Naser, J.; Mjalli F. S.; Gano, Z. S., Molar heat capacity of tetrabutylammonium chloride-based deep eutectic solvents and their binary water mixtures, Asia-Pac. *J. Chem. Eng.,* **2017**, *12*, 938-947, DOI: 10.1002/apj.2130.

[32] Zarei, F.; Rahimi, M. R.; Razavi, R.; Baghban, A., Insight into the experimental and modeling study of process intensification for post-combustion CO_2 capture by rotating packed bed, *J. Clean. Prod.,* **2019**, *211*, 953-961, DOI: 10.1016/j.jclepro.2018.11.239.